Nigerian Journal of Technology (NIJOTECH)
Vol. 39, No. 2, April 2020, pp. **579 – 588**

Print ISSN: 0331-8443, Electronic ISSN: 2467-8821
www.nijotech.com
http://dx.doi.org/10.4314/njt.v39i2.29

OIL SPILL IDENTIFICATION IN VISIBLE SENSOR IMAGING USING AUTOMATED CROSS CORRELATION WITH CRUDE OIL IMAGE FILTERS

G. Ofualagba[1] and D. U. Onyishi[2,*]
[1, 2,] FEDERAL UNIVERSITY OF PETROLEUM RESOURCES (FUPRE), P.M.B. 1221, EFFURUN, DELTA STATE, NIGERIA
E-mail addresses: [1] *ofualagba.godswill@fupre.edu.ng*, [2] *onyishi.donatus@fupre.edu.ng*

ABSTRACT
An algorithm for detection of crude oil spills in visible light images has been developed and tested on 50 documented crude oil spill images from Shell Petroleum Development Company (SPDC) Nigeria. A set of three 25 x 25 pixels crude oil filters, with unique red, green, and blue (RGB) colour values, homogeneity, and power spectrum density (PSD) features were cross-correlated with the documented spill images. The final crude oil spill Region of Interest (ROI) was determined by grouping interconnected pixels based on their proximity, and only selecting ROIs with an area greater than 5,000 pixels. The crude oil filter cross correlation algorithm demonstrated a sensitivity of 84% with a False Positive per Image (FPI) of 0.82. Future work includes volume estimation of detected spills using crude oil filters, and utilizing this information in the recommendation of appropriate spill clean-up and remediation procedures for the detected spills.

Keywords: *Crude Oil Spill Detection, Crude oil image filters, Cross correlation, Visible sensor imaging, Oil Spill Segmentation.*

1. INTRODUCTION

Land crude oil spills prevent soil aeration, affect soil temperature, structure, fertility, and pH. It is also responsible for the contamination of ground water. Crude oil spills are responsible for the destruction of soil microorganisms and agricultural crops. This leads to severe reduction in fishing and farming activities and results in poverty and regional underdevelopment [1]. The public expectation is that oil spill extent and locations are precisely mapped to implement countermeasures to minimize the effect of pollution [10].

Several methods have been employed for spill detection, including real-time remote surveillance by flying aircrafts with surveillance teams. Other methods employ various sensors such as visible sensors, infrared sensors, ultraviolet sensors, radar sensors, and laser fluorosensor. A lot of emphasis has been placed on sea oil pollution and the use of synthetic aperture radar (SAR) imaging by satellites for remote sensing, mapping and monitoring of marine oil spills [11-14]. The detection of oil spills using SAR images are divided into stages: pre-processing of the images, segmentation, feature extraction; oil spill and look-alike discrimination; and classification of dark spots which potentially correspond to oil spills [11, 13, 15-18]. Most spill detection algorithms have been developed specifically for SAR imaging. However, video cameras are used extensively for oil spill monitoring, especially on land crude oil spills, and Light-enhanced video cameras function in complete darkness. The visible light spectrum still remains a research area as an economical method for monitoring oil spills, particularly on countermeasures support operations [10].

Shell Petroleum Development Company (SPDC) Nigeria regularly captures visible light images of all land crude oil spills detected by the company and utilizes this in data gathering for spill response, clean-up and remediation measures [19]. Automated oil spill surveillance systems, such as the Ground Robotic Oil Spill Surveillance (GROSS) system [20-21], the Aerial

*** Corresponding author, tel: +234 – 803 – 432 – 1196**

Spill Surveillance System [22], and the Underwater Oil Spill Surveillance (UROSS) System [23-24] employ the use of visible light sensors when reporting the parameters of a detected crude oil spill. It is therefore necessary that oil spill detection algorithms for land crude oil spills be developed to be employed for economical monitoring and detection of crude oil spills on land.

This paper presents an algorithm to detect the presence of land crude oil spills automatically in images acquired using visible light sensors. A set of three 25 by 25 pixels crude oil filters were designed and developed from land crude oil spill images obtained by SPDC [19]. A set of documented images of land crude oil spills which occurred in the Niger Delta region of Nigeria in 2019, were obtained from SPDC [19]. Automatic cross-correlation of the crude oil filters with documented land crude oil spill images was performed and the ability to detect land crude oil spills using these filters was evaluated. The effect of darkness, cloud cover, and sun glitter, and oil sheen, on the efficacy of the crude oil filters are analyzed subsequently.

2. METHODS

A set of three crude oil filters were developed from the oil spill images documented by SPDC Nigeria over the years [19]. They were labeled as crudeoilfilter1, crudeoilfilter2, and crudeoilfilter3 respectively. Each oil filter had a specific RGB value associated with the crude oil colour found in the documented spill images by SPDC, as well as distinguishing homogeneity and power spectrum density (PSD) texture features. Homogeneity is a measure of how close in the grayscale values of a pixel is when compared with its neighbouring pixels. The power spectrum density (PSD) shows the strength of the variations (energy) as a function of frequency. It provides a representation of the amplitude of a surface's roughness as a function of the spatial frequency of the roughness.

A block diagram of the image processing algorithm employed in this paper is depicted in Figure 2. The algorithm was developed and tested using MATLAB™ (The Mathworks™, Natick, MA, USA). Fifty (50) images of documented crude oil spills in the Niger Delta region of Nigeria in 2019 by SPDC were obtained from SPDC [19]. Image pre-processing was done to remove the label pixels at the bottom of each image [1]. Next, each crude oil filter was cross-correlated with each crude oil filter in three phases: colour cross correlation, homogeneity cross correlation, and PSD cross correlation.

For the colour cross correlation, the average red (R), green (G), and blue (values) for the 25 by 25 pixels image block being processed was computed and compared with the RGB value of the crude oil filter. If the difference between the image block RGB value and the crude oil filter's RGB value was greater than an experimentally determined threshold, C_T, then the image block was classified as being crude-oil free. If the difference was within C_T, then the image block was classified as having the potential to contain a crude oil spill, and the image block was passed on to the second stage for further analysis.

In the second stage homogeneity cross correlation was performed with the grayscale images of the crude oil filters and the documented crude oil spill image. Using a window size of 3 x 3 pixels, the homogeneity for each pixel in the image block was computed. If the difference between the average grayscale value of the nine pixels in the window and the grayscale value of the centre pixel is within a small range, then the central pixel is classified as a homogeneous pixel.

(a) (b) (c)

Figure 1: Crude Oil Filters designed and developed using documented crude oil spill images by SPDC.

Using this method, the percentage of homogeneity in each 25 x 25 pixels image block was determined and compared with the homogeneity percentage of the crude oil filter. If the difference in homogeneity percentage of the image block and the crude oil filter was greater than 2%, then the image block was classified as being crude oil free and no further processing was performed on the block. However, if the difference in homogeneity percentage of the image block and the crude oil filter was less than 2%, then that image block was classified as having the potential to contain a crude oil spill and passed on to the third stage for further analysis.

In the third stage, the power spectrum density (PSD) for the image block was computed using the equation (1):

$$PSD = \log_{10}(abs(fftshift(fft2(ROI)))^2) \quad (1)$$

where *ROI* is the current 2-dimensional grayscale image block being processed, *fft2* is the two-dimensional Fast Fourier Transform (FFT) of the image block, *fftshift* rearranges the Fourier Transform of ROI by shifting the zero-frequency component to the centre of the array., and *abs* is the absolute value obtained for each pixel computation. If the difference between the average PSD of the image block and the crude oil filter was greater than a certain threshold, PSD_T, then the image block was classified as being crude oil free. If the difference between the average PSD for the 25 x 25 image block and the crude oil filter was within PSD_T, then that image block was classified as having crude oil spill and selected as a Region of Interest (ROI).

This cross-correlation process was repeated across the entire documented crude oil spill image with each of the three crude oil filters, and crude oil spill ROIs extracted by each filter were integrated into a final image containing regions flagged as crude oil spills. The final crude oil spill ROI was determined by grouping interconnected pixels based on their grayscale values and proximity to one another. ROIs with an area greater than 5,000 pixels (i.e. > 8 interconnected 25 x 25 image blocks) were selected as successful spill detection. ROIs with areas less than 5,000 pixels were discarded in the final spill detection image output by the algorithm.

A sample of the developed algorithm in MATLAB that was used to run tests on the 50 documented crude oil spill images obtained from SPDC is shown in the Appendix.

It should be noted that the section of the algorithm presented above performs automated cross correlation of crude oil spill images with crudeoilfilter1. However, the full algorithm written and tested performs the automated cross correlation of the crude oil spill images with crudeoilfilter1, crudeoilfilter2, and crudeoilfilter3. The results obtained from running this algorithm on 50 crude oil spill images documented by SPDC are presented in the Results Section.

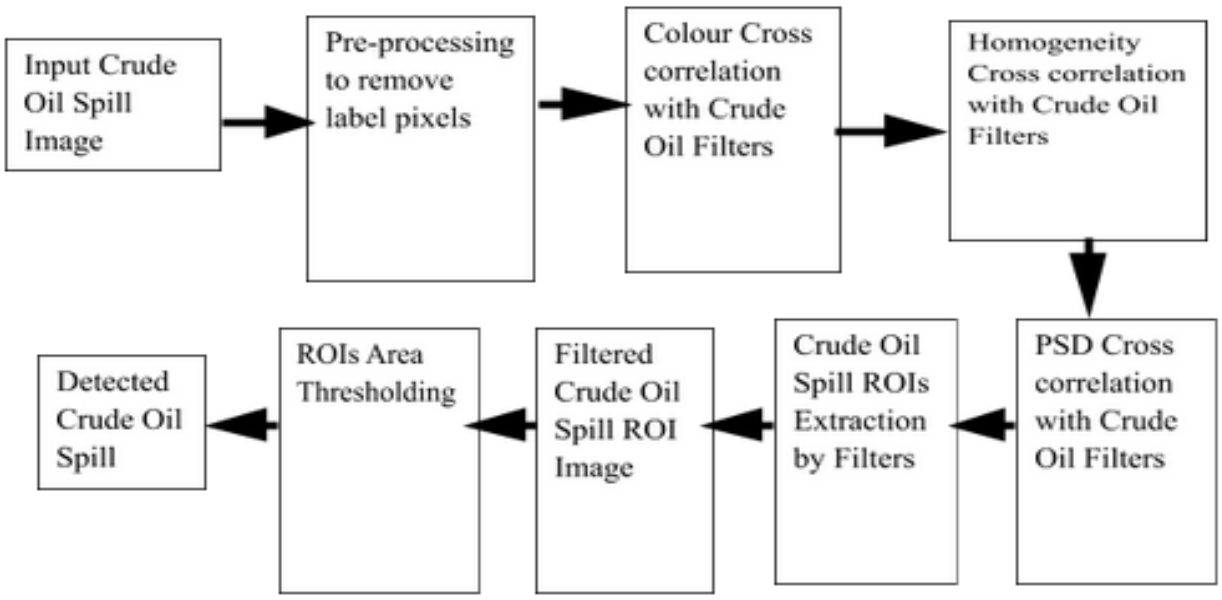

Figure 2. Block Diagram of the Crude oil filter cross correlation algorithm for Crude Oil Spill Detection.

3. RESULTS

Figure 3 shows the output of the crude oil filter cross correlation algorithm implemented on a documented crude oil spill image from SPDC [19]. Figure 3a shows the original image containing the documented crude oil spill. Figure 3b shows the pre-processed image in which the label pixels at the bottom have been removed prior to performing cross correlation. Figure 3c shows the output of the algorithm after cross correlation has been performed on image in 3b using crudeoilfilter1. Figure 3d shows the output of the algorithm after cross correlation has been performed on image in figure 3b using crudeoilfilter2. Figure 3e shows the output of the algorithm after cross correlation has been performed on image in 3b using crudeoilfilter3. Figure 3f shows the integrated final image containing all ROIs flagged as having crude oil. ROI Area thresholding is performed on Figure 3f and the final result of the detected crude oil spill is shown in Figure 3g.

The crude oil filter cross correlation algorithm was tested on 50 documented spill images from SPDC [19]. The results are presented in Table 1. The algorithm successfully detected the crude oil spill in 42 out of 50 images, resulting in an overall sensitivity of 84%. False Positives (FPs) were counted by visually identify regions in the algorithm's output image which did not contain crude oil spills, but which the algorithm wrongly classified as crude oil spills. This count represents the specificity of the algorithm's ability to correctly classify only crude oil spills as crude oil spills. For the 50 images, the algorithm was tested on; the average False Positive per Image (FPI) was 0.82. In other words, for every crude oil spill image, the algorithm incorrectly flags less than 1 region (0.82) as a crude oil spill. The maximum number of False Positives for a Crude Oil Spill Image was 4.

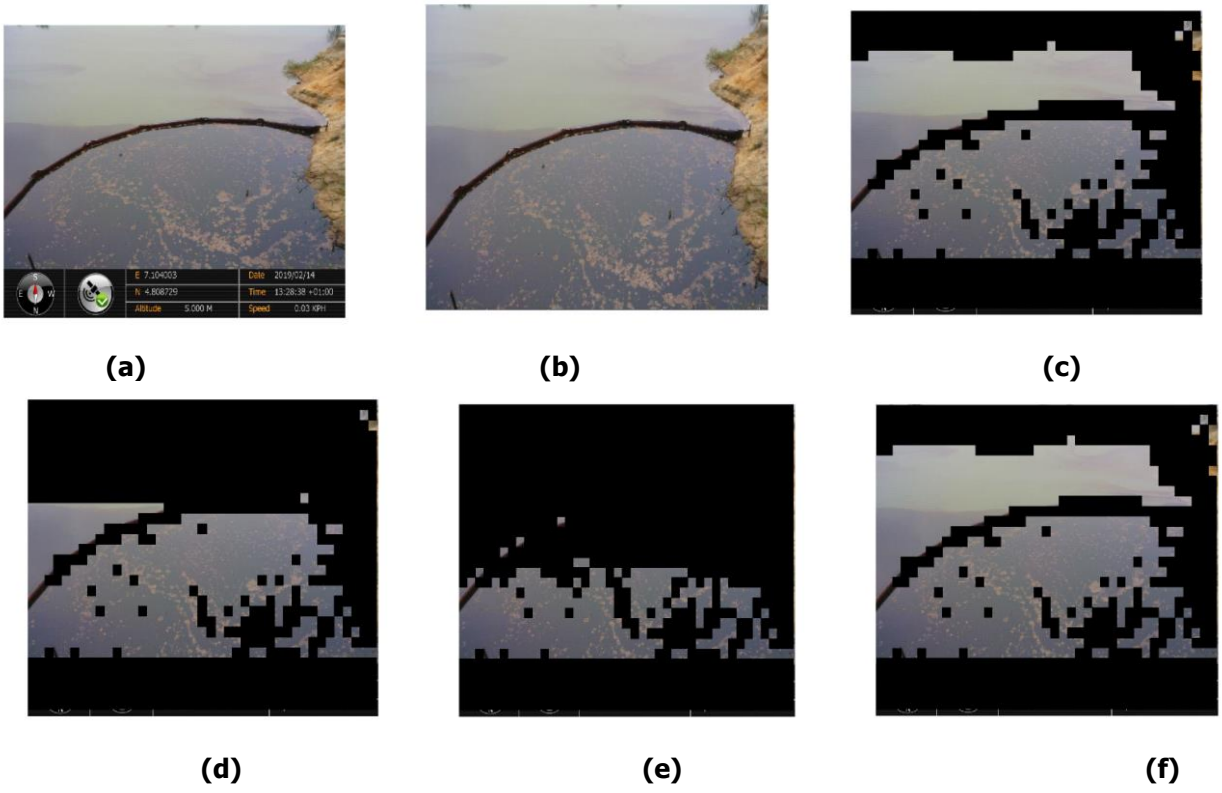

(a) **(b)** **(c)**

(d) **(e)** **(f)**

(g)

Figure 3: Crude Oil Filter Cross Correlation Algorithm Results. (a) Documented Crude Oil Spill Image. (b) Pre-processed Image. (c) Spill Detected by crudeoilfilter1 (d) Spill detected by crudeoilfilter2 (e) Spill detected by crudeoilfilter3 (f) Final integrated image of spill detected by the 3 filters (g) Area thresholded image from (f) yielding detected oil spill.

Table 1: Results of the Crude Oil Filter Cross Correlation Algorithm on 50 documented crude oil spill images from SPDC [11].

Spill Image No	Detected Spill	No of False Positives (FP)
1	NO	0
2	YES	4
3	YES	0
4	YES	0
5	YES	1
6	YES	0
7	YES	1
8	YES	1
9	YES	1
10	YES	1
11	YES	3
12	NO	0
13	YES	0
14	YES	0
15	NO	0
16	YES	1
17	YES	1
18	YES	0
19	YES	2
20	YES	0
21	YES	1
22	YES	0
23	NO	1
24	YES	1
25	YES	3
26	YES	1
27	YES	0
28	YES	2
29	YES	0
30	NO	0
31	YES	1
32	YES	0
33	YES	0
34	NO	0
35	YES	3
36	YES	0
37	YES	1
38	YES	2
39	NO	0
40	YES	2
41	NO	0
42	YES	1
43	YES	4
44	YES	1
45	YES	0
46	YES	0
47	YES	1
48	YES	0
49	YES	0
50	YES	0

4. DISCUSSION

The crude oil filter cross correlation algorithm demonstrated the ability to eliminate existing vegetation due to low correlation in homogeneity and colour. The algorithm was also successful in eliminating the sky portion present in the crude oil spill images due to low colour template matching between the sky pixels and the crude oil filters. This is shown in Figure 4.

In several cases where the algorithm failed to successfully detect the presence of crude oil spill in the image, the reason for the algorithm's failure could be attributed to sun glitter on the spill (see Figures 4a & 4b). Direct sunlight intensity on the spill caused the RGB colour of the crude oil to be outside the RGB range of the crude oil filters and so thereby rendered such spills undetectable by the algorithm.

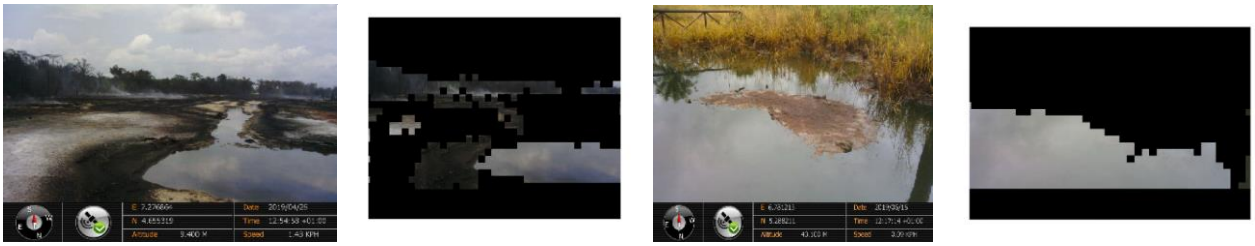

(a) (b) (c) (d)

Figure 4: Sky and Vegetation Discrimination by crude oil filter cross correlation algorithm. (a) Documented Spill Image 11; (b) Detected spill in Image 11 with elimination of sky pixels; (c) Documented Spill Image 33; (d) Detected spill in Image 33 with elimination of vegetation pixels.

There were several documented spill images that contained smoke and burning fire, which resulted in the algorithm wrongly flagging them as crude oil spills (see Figures 4c & 4d). Extra features may need to be incorporated into the crude oil filters to enable them to accurately identify and eliminate fires and smoke while detecting crude oil spills.

In addition to failure to detect spills due to sun glitter, it was also observed that in some cases, the algorithm was unable to fully detect crude oil spills that had oil sheen on the surface (see Figures 4e & 4f). Furthermore, in some cases, the algorithm only detected a fraction of the spilled crude volume (see Figures 4 g & 4h). This was due to the limited RGB range of the three oil filters used for cross correlation. Only three crude oil filters were employed to achieve a sensitivity of 84% with an FPI of 0.82. There is need to develop and use more crude oil filters to improve the efficiency and accuracy of the algorithm. The size of the crude oil filters utilized in the work was 25 x 25 pixels. There is need to find the optimal filter size that will perform best in crude oil spill detection. Future work includes volume estimation of detected spills and utilizing this information for recommending appropriate spill clean-up and remediation procedures for the detected spill.

In the development of this spill detection algorithm for visible sensor images, the authors utilized documented crude oil spill images from SPDC [19], because currently there does not exist a publicly available database of calibrated crude oil spill images using visible sensors for researchers to utilize in developing spill detection algorithms for visible images. It is possible to obtain SAR images from satellites to assist in the developing of detection algorithms for SAR images. However, since video cameras are used extensively for oil spill monitoring, especially on land crude oil spills, and the visible light spectrum still remains a research area as an economical method for monitoring oil spills, the authors recommend that a public database containing calibrated crude oil spill images be developed and made available for researchers to have access and be able to develop successful spill detection algorithms for images in the visible spectrum.

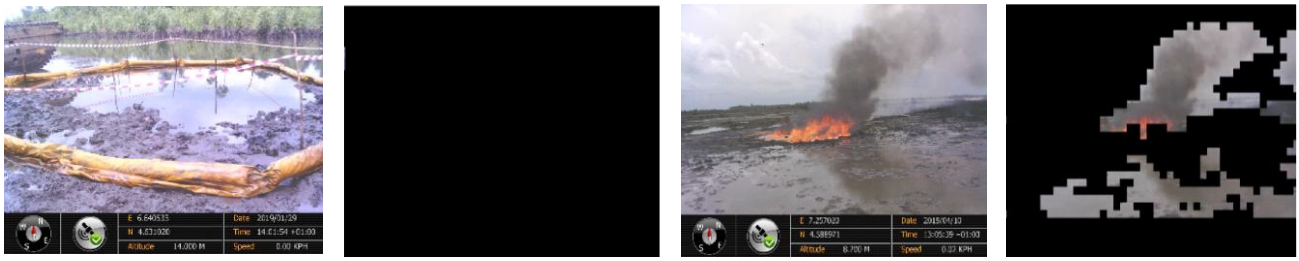

(a) (b) (c) (d)

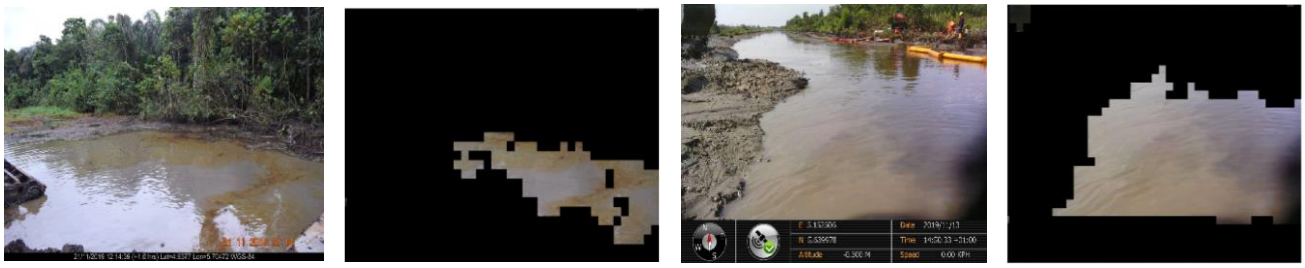

(e) (f) (g) (h)

Figure 4. Factors affecting sensitivity and specificity of the crude oil filter cross correlation algorithm. (a) Documented Spill Image 1; (b) Non-detected spill in Image 2 due to direct sunlight intensity on spill; (c) Documented Spill Image 16; (d) False Positive (FP) due to smoke and fire; (e) Documented Spill Image 50; (f) Partially detected spill in Image 50 due to oil sheen; (g) Documented Spill Image 46; (h) Partially detected spill in Image 46 due to narrow RGB of crude oil filters.

6. CONCLUSION

A set of 25 x 25 crude oil filters with unique RGB, homogeneity and power spectrum density features have been developed and tested. The filters were applied to 50 documented Crude Oil Spill Images from the Niger Delta region of Nigeria. The crude oil filters demonstrated the ability to successfully detect crude oil spills in 42 of the 50 images (an efficiency of 84%) with an FPI of 0.82. Crude oil filters spill detection is affected by sunlight intensity, presence of oil sheen, and the presence of smoke and burning fires in the images. Future work includes volume estimation of detected spills using crude oil filters, and utilizing this information in the recommendation of appropriate spill clean-up and remediation procedures for the detected spills.

7. REFERENCES

[1] Ejofodomi, O. and Ofualagba, G., "Detection and Classification of Land Crude Oil Spills Using Color Segmentation and Texture Analysis", *Journal of Imaging*, Vol. 3, Issue 4, (47), pp 1-21, 2017.

[2] Oyebamiji M., Adekola Mba, Igwe C., 2014. Effects of Oil Spillage on Community Development in the Niger Delta Region: Implications for the Eradication of Poverty and Hunger (Millennium Development Goal One) in Nigeria. *World Journal of Social Science*, Vol. 1, No. 1, 27-36.

[3] Ahmadu J and Egbodion J (2013). Effect of oil spillage on cassava production in Niger delta region of Nigeria. *American J Experimental Agriculture* 3: 914-926.

[4] Iwejingi SF (2013). Socio-economic problems of oil exploration and exploitation in Nigeria's Niger delta. J Energy Technologies and Policy 3: 76-80.

[5] Osuagwu E. S., Olaifa E., 2018. Effects of oil spills on fish production in the Niger Delta. *PLoS ONE* 13(10), 1 -14.

[6] Frank O., Boisa N., 2018. The effect of crude oil spill on the surface water of the Lower Niger Delta (Sombriero River). J Ind Environ Chem. 2(2),19-24.

[7] Oshienemen N., Albert, Dilanthi Amaratunga, Richard P. Haigh, 2018. Evaluation of the Impacts of Oil Spill Disaster on Communities and Its Influence on Restiveness in Niger Delta, Nigeria. Procedia Engineering, 212, 1054-1061. https://doi.org/10.1016/j.proeng.2018.01.136

[8] A. Fentiman, N. Zabbey, 2015. Environmental degradation and cultural erosion in Ogoniland: A case study of the oil spills in Bodo. The Extractive Industries and Society, 2(4), 615-624.

[9] Oyebamiji M., Adekola Mba, Igwe C., 2014. Effects of Oil Spillage on Community Development in the Niger Delta Region: Implications for the Eradication of Poverty and Hunger (Millennium Development Goal One) in Nigeria. World Journal of Social Science, Vol. 1, No. 1, 27-36.

[10] Merv, F. and Carl, E. B., "A Review of Oil Spill Remote Sensing Sensors", *Sensors* Vol.18, Issue 1,(91), 2018.

[11] Cantorna, D., Dafonte, C., Iglesias, A. and Arcay, B, "Oil spill segmentation in SAR images using convolutional neural networks. A comparative analysis with clustering and logistic regression algorithms", *Applied Soft Computing Journal,* Vol.84, (105719), pp.1-13, 2019.

[12] Chen, G., Li, Y., Sun, G and Zhang, Y., "Application of Deep Networks to Oil Spill Detection Using Polarimetric Synthetic Aperture Radar Images", *Applied Sciences*, Vol. 7, (968), 2017.

[13] Krestenitis, M., Orfanidis, G., Ioannidis, K., Avgerinakis, K., Vrochidis, S. and Kompatsiaris, I., "Oil Spill Identification from Satellite Images Using Deep Neural Networks Remote Sensing", *Remote Sensing,* 11(15), 1762.2, 2019.

[14] Ferraro G., Meyer-Roux S., Muellenhoff, O., Pavliha M., Svetak J., Tarchi D. and Topouzelis K., "Long term monitoring of oil spills in European seas". *International Journal of Remote Sensing, 30(3)*, pp. 627–645, 2009.

[15] Kolokoussis, P. and Karathanassi, V., "Oil Spill Detection and Mapping Using Sentinel 2 Imagery", *Journal of Marine Science and Engineering,* Vol. 6(4), pp. 1-12, 2018.

[16] Lang H., Zhang X., Xi Y., Zhang X. and Li W., "Dark-spot segmentation for oil spill detection based on multi-feature fusion classification in single-pol synthetic aperture radar imagery", *Journal of Applied Remote Sensing*, Vol. 11, pp. 015006, 2017.

[17] Su T.F., Li H.Y.; Liu T.X., "Sea Oil Spill Detection Method Using SAR Imagery Combined with Object-Based Image Analysis and Fuzzy Logic", *Advanced Materials Research,* Volumes 1065–1069, pp. 3192–3200, 2015.

[18] Chen, Z., Wang, C. and Teng, X., "Oil spill detection based on a superpixel segmentation method for SAR image", *In Proceedings of the2014 IEEE International Geoscience and Remote Sensing Symposium (IGARSS), Quebec City, QC, Canada,* 13–18 July 2014.

[19] Shell Nigeria. Available online: www.shell.com.ng (accessed on January 27, 2020).

[20] Ejofodomi, O., Ofualagba, G., "Exploring the Feasibility of Robotic Pipelilne Surveillance for Detecting Crude Oil Spills in the Niger Delta", *International Journal Unmanned System Engineering,* Vol. 5, pp. 8–52, 2017.

[21] Ejofodomi, O. and Ofualagba, G., "Ground Robotic Oil Spill Surveillance (GROSS) System for Early Detection of Oil Spills from Crude Oil Pipelines", *International Journal of Imaging & Robotics,* Vol. 20, No. 2, 2020.

[22] Ejofodomi, O. and Ofualagba, G., "Development of an Aerial Robotic Oil Spill Surveillance (AROSS) System for Constant Surveillance and Detection of Spills from Crude Oil Pipelines", *International Journal of Unmanned System Engineering*, Vol.4,pp.19-33, 2016.

[23] Ejofodomi O. A. and Ofualagba G., "Design of an Underwater Robotic Oil Spill Surveillance (UROSS) System for Surveillance and Detection of Spills from Subsea Crude Oil Pipelines", *International Journal of Unmanned System Engineering* Vol. 6, No. 1, pp. 1-20, 2018.

[24] Ejofodomi, O. and Ofualagba, G., "Subsea Crude Oil Spill Detection Using Robotic Systems", *European Journal of Engineering Research and Science*, Vol. 4(12), pp. 112-116, 2019.

APPENDIX: SAMPLE AGORITHM OF DOCUMENTED CRUDE OIL SPILL IMAGES

```
% read in original documented crude oil spill image
A = imread('IMG_20200218_095108.jpg');

% perform image pre-processing to remove label pixels in the image.
B = A(1: labelrow, 1:labelheight,:);

% load the three crude oil filters designed and developed from
% documented spill images
oilfilter1 = imread('OSFILTER1.jpg');
oilfilter2 = imread('OSFILTER2.jpg');
oilfilter3 = imread('OSFILTER3.jpg');

[aa bb cc] = size(B);
C = rgb2gray(B);
D = B

for i=1:25:aa
  for j=1: 25:bb

     % Performing Color Cross Correlation
          averageR = mean(mean(B(i:i+25,j:j+25,1)));
```

```
        averageG = mean(mean(B(i:i+25,j:j+25,2)));
        averageB = mean(mean(B(i:i+25,j:j+25,3)));

        if(((abs(averageR - oilfilter1R)) > Ct) && ((abs(averageG - oilfilter1G)) > Ct) &&  ((abs(averageB - oilfilter1B)) > Ct))
         count = 0;

                % Performing Homogeneity Correlation
                for k=i:i+25
                for l=j:j+25
   homogeneity = ((C(k,k) + C(k-1,l) + C(k+1,l) + C(k,l-1) + C(k-1,l-1) + C(k+1,l-1) + C(k,l+1) + C(k-1,l+1) + C(k+1,l+1))/9);
                if(abs((C(k,l)) - homogeneity) < Ht)
     hcount++;
                end
                end
                end

                hpercent = hcount/(25*25);
                if((abs(hpercent - oilfilter1hpercent)) < 2)

                        % Performing Power Spectrum Density Cross Correlation
                        PSD = log10(abs(fftshift(fft2(C(i:i+25,j:j+25))))^2);

                        if( abs(max(max(PSD) - max(max(oilfilter1PSD)))                 < PSDt)
                                % leave this image block as it contains crude             % oil spill
                        else
                                for k=i:i+25
                                for l=j:j+25
                                D(k,l,1) = 0;
                                    D(k,l,2) = 0;
                                    D(k,l,3) = 0;
                                end
                                end
                        end
                else
                        for k=i:i+25
                        for l=j:j+25
                        D(k,l,1) = 0;
                                D(k,l,2) = 0;
                                D(k,l,3) = 0;
                        end
                        end

        end

        else
                for k=i:i+25
                for l=j:j+25
                D(k,l,1) = 0;
                        D(k,l,2) = 0;
                        D(k,l,3) = 0;
                end
                end
end
```

```
 end
end

% connect neighboring pixels that contain crude oil spills
E = rgb2gray(D);
Spillimage = bwlabel(E);
stats = regionprops(Himage,'Area');

% select only pixel groups with sizes greater than 5,000 pixels
idx = find([stats.Area] > 5000);
CC= bwconncomp(Spillimage);
BW2 = ismember(labelmatrix(CC), idx);

% display final crude oil spill image with detected crude oil spills
F = B;
for i=1:aa
   for j=1:bb
      if(BW2(i,j) > 0)
      else
         F(i,j,1) = 0; F(i,j,2) = 0; F(i,j,3) = 0;
      end
   end
end
figure;imshow(F);hold on;
title('Detected Crude Oil Spill');
```